# The kinase Greatwall phosphorylates an inhibitor of protein phosphatase 2A that is essential for mitosis

Satoru Mochida[1,2], Sarah L. Maslen[1], Mark Skehel[1] & Tim Hunt[1]*

1, Cancer Research UK,

London Research Institute,

Clare Hall Laboratories,

South Mimms,

Herts EN6 3LD,

United Kingdom.

2, Priority Organization for Innovation and Excellence,

Kumamoto University,

2-2-1 Honjo,

Kumamoto,

Kumamoto 860-0811,

Japan.

*Corresponding author: tim.hunt@cancer.org.uk.

**Entry into mitosis in eukaryotes requires the activity of Cyclin-dependent kinase 1 (CDK1). CDK1 is opposed by protein phosphatases in two ways: they inhibit its activation by dephosphorylating the protein kinases Wee1 and Myt1 and the protein phosphatase Cdc25 (key regulators of Cdk1) and they also antagonize its own phosphorylation of downstream targets. A particular form of protein phosphatase 2A (PP2A) containing a B55δ subunit is the major protein phosphatase that acts on model CDK substrates in *Xenopus* egg extracts and has anti-mitotic activity. The activity of PP2A-B55δ is high in interphase and low in mitosis, exactly opposite to that of CDK1. We report that inhibition of PP2A-B55δ results from a small protein known as α-Endosulfine (Ensa), which is phosphorylated in mitosis by the protein kinase Greatwall (Gwl). This converts Ensa into a potent and specific inhibitor of PP2A-B55δ. This pathway represents a new element in the control of mitosis.**

Progression from interphase to mitosis requires a large number of proteins to be phosphorylated to bring about processes such as nuclear envelope breakdown, chromosome condensation and spindle assembly (*1*). Cyclin dependent kinase 1 (Cdk1)-cyclin B, also called maturation-promoting factor (MPF), is the main (but not the sole) protein kinase that catalyzes these modifications (*2*). The activation of MPF requires that Cdc25, a phosphatase for the phospho-$Tyr^{15}$ residue of Cdk1, is active, whereas Wee1 and Myt1, the protein kinases that phosphorylate $Tyr^{15}$, must be turned off. This is achieved by multisite phosphorylation of both Cdc25 and Wee1 and Myt1 (*3-5*), mainly catalysed by MPF itself (*6*), and opposed by protein phosphatase 2A (PP2A)-B55δ (*7*). This form of PP2A is a major phosphatase for model CDK substrates (*8*), and depletion of PP2A-B55δ accelerates mitotic progression in

*Xenopus* extracts (*8*), partly by promoting the activity of Cdc25 and the inactivity of Wee1 and Myt1 and partly by reducing antagonising phosphatase activity against the substrates of CDKs and other mitotic kinases (*9*). Crucially, the activity of PP2A-B55δ fluctuates during the cell cycle, being high in interphase and low in mitosis (*10*). This presumably accentuates the switchlike behaviour of the system; when a kinase is active, the opposing phosphatase is inactive and *vice versa*. This behaviour also avoids futile cycles. But how PP2A-B55δ phosphatase is regulated was not known.

An important clue to the control of PP2A-B55δ has recently emerged from studies of the protein kinase Gwl (*11*). In *Xenopus* egg extracts, Gwl is activated in mitosis and is essential both for entry into mitosis and for maintenance of the mitotic state (*11*). Gwl apparently promotes mitosis by inactivating PP2A (*9, 12*). We were unable to detect significant phosphorylation of the components of PP2A-B55δ *in vitro* (also observed by M. Goldberg, personal communication), and therefore suspected that Gwl might rather act by phosphorylating and activating some as-yet unidentified PP2A-B55δ-specific inhibitor protein. We therefore searched for Gwl substrates with the KESTREL method (*13*) in which active Gwl was incubated with extracts containing potential substrates, under conditions where endogenous protein kinase activity was suppressed. Several proteins in interphase egg extracts were phosphorylated by Gwl (Fig. 1A), and two prominent substrates of small apparent molecular size (arrowed) were heat-stable. The boiled extract was fractionated on a Mono-Q column and fractions containing the major substrate were analysed by mass spectrometry. About 80 different *Xenopus* proteins were detected, but no Gwl-dependent phosphorylated peptides emerged from the analysis. So we choose 29

proteins with molecular sizes between 10 and 30 kilodaltons from the list and expressed them in bacteria (Fig. 1B). Seventeen of them were soluble after boiling and these were further tested as substrates for Gwl *in vitro*. One protein, cyclic AMP-regulated phosphoprotein-19 (ARPP-19), was a better substrate for Gwl than any of the others (Fig 1B, lane 22). ARPP-19 is a major substrate for cAMP-activated protein kinase (PKA) in post-synaptic neurons (*14*). ARPP-19 is a close relative of α-endosulfine (Fig. 1C), which was identified as an endogenous ligand of sulfonylurea receptor $K^+$ channels in pancreas (*15*) although this idea seems to have been abandoned by its original proponents (*16*). Recombinant Ensa, like ARPP-19, was a good substrate for Gwl. Substitution of alanine for all the potential conserved phosphorylation sites in ARPP-19 and Ensa (11 in the former and 7 in the latter) abolished phosphorylation by Gwl (Fig. 1D and Fig. S1). By contrast, mutants of ARPP-19 and of Ensa that retained Ser67 in the highly conserved sequence FDSGDY were phosphorylated by Gwl to a similar degree as were the wild-type proteins. As these proteins also have conserved CDK (S/T-P-X-K/R) and PKA (K/R-K/R-X/S/T) consensus sites, we tested if they were substrates for these kinases *in vitro*. Indeed, $Ser^{28}$ of ARPP-19 and $Thr^{28}$ of Ensa were strongly (and $Thr^{99}$ residues of both proteins weakly) phosphorylated by CDK2-cyclin A. $Ser^{109}$ of both proteins was the major site targeted by PKA (Fig. 1D and Fig. S1A) (*17*).

We raised antibodies against ARPP-19 and Ensa in rabbits and used them to measure the concentrations of ARPP-19 and Ensa in *Xenopus* egg extracts. ARPP-19 was hardly detectable despite its presence in the original mass spectrometric analysis. On the other hand, Ensa was present at about 150-300 nM in egg extracts, in excess of PP2A-B55δ, whose concentration we measured at about 50~70 nM.

We tested whether Ensa affected the phosphatase activity of PP2A-B55δ. Although dephosphorylated Ensa did not inhibit any form of PP2A, Ensa phosphorylated by Gwl strongly inhibited the PP2A-B55δ hetero-trimer holocomplex (Fig. 2A), but not the monomeric catalytic subunit or the AC dimer. Phosphorylation of Ensa by CDK or PKA had little effect on its inhibitory activity only by itself. Similar results were obtained for ARPP-19 (Fig. S1B). These results indicate that ARPP-19 and Ensa are converted into inhibitors of PP2A-B55δ by phosphorylation on $Ser^{67}$.

We tested the specificity of Ensa's interactions with various forms of PP2A and other protein phosphatases by making affinity matrices covalently conjugated with Ensa. Gwl-phosphorylated Ensa strongly bound PP2A-B55δ from interphase egg extracts, but no other B subunits nor the PP1 or PP5 catalytic subunit were retained by Ensa beads (Fig. 2B). Mock- and PKA-phosphorylated Ensa bound PP2A-B55δ only weakly. These results suggest that Ensa inhibits PP2A-B55δ by a $Ser^{67}$ phosphorylation-dependent physical interaction, which makes it a highly specific inhibitor of PP2A-B55δ. Neither Ensa nor ARPP-19 inhibited PP1, regardless of their phosphorylation state (Fig. S1C).

Anti-phospho-$Ser^{67}$-specific antibodies reacted with Ensa in mitotic extracts much more strongly than in interphase extracts (Fig. 3A). Using Phos-tag™ acrylamide gels, which specifically retard phosphorylated proteins (*18*), we confirmed that the majority of Ensa became phosphorylated in mitotic extracts (Fig. 3A) and that $Ser^{67}$ was required for the observed phosphorylation-dependent shift in migration on

polyacrylamide gel electrophoresis (Fig. 3A). These results show that Ensa is quantitatively phosphorylated at its $Ser^{67}$ residue in mitosis, which leads to the inhibition of PP2A-B55δ. The timing of Ensa phosphorylation in relation to that of a number of other cell cycle markers in shown in Fig. S2. The phosphorylation of anaphase-promoting complex-3 (Apc3), Cdc25, Wee1 and Gwl all took place at the same time at the resolution of this experiment.

We tested the effects of Ensa depletion on 'cycling' frog egg extracts. In this experiment, the control (Fig. 3C) performed two cycles of entry into and exit from mitosis, whereas the Ensa-depleted extract (Fig. 3D) never entered M-phase despite larger amounts of histone H1 kinase activity than in the control. Apc3 was never fully phosphorylated, and mitotic phosphoproteins showed only slightly increased intensity (Fig. S3C). Cyclin destruction was not activated in the Ensa-depleted extract. Adding back wild-type recombinant Ensa to depleted extracts restored induction of mitosis (Fig. 3E) whereas the $Ser^{67}$Ala mutant protein did not (Fig. S3A), indicating that $Ser^{67}$ of Ensa is crucial for proper cell cycle control. $Tyr^{15}$ of Cdk1 was dephosphorylated in all three conditions, but in the Ensa-depleted extract, $Tyr^{15}$ remained dephosphorylated for the duration of the incubation, whereas in the controls, $Tyr^{15}$ was rephosphorylated. This experiment implies that the main effect of not inhibiting PP2A-B55 is in antagonising Cdk1 phosphorylation of downstream target proteins, rather than on the control of Cdk1 activity. Somehow, Cdc25 or an equivalent activity that dephosphorylated $Tyr^{15}$ was activated in the Ensa-depleted extract, yet despite strong histone H1 kinase activity, the extract failed to enter mitosis.

We tested the results of adding thiophosphorylated Ensa to egg extracts. Fig. S4 shows that when extra Ensa was added to interphase extracts supplemented with cycloheximide and a small amount of recombinant stable cyclin B (not enough to induce mitosis by itself), phosphorylation events typical of mitotic extracts were induced when Gwl-thiophosphorylated Ensa was added. Dephosphorylated Ensa or Ensa thiophosphorylated by PKA did not show any effect. These results are all consistent with the idea that Gwl inhibits PP2A-B55δ by phosphorylating Ensa, thereby both activating CDK1 (by inhibiting Wee1 and turning on Cdc25) and allowing CDK1 to efficiently phosphorylate its target proteins in mitosis by suppressing the activity of the main opposing protein phosphatase.

In this paper we identify Ensa and ARPP-19 as phosphorylation-dependent inhibitors of PP2A-B55 and physiological substrates of Gwl kinase. In *Drosophila* Ensa is required for proper spindle assembly and oocyte maturation; endosulfine-deficient oocytes are unable to pass between prophase of first meiosis into metaphase (*19-21*). Tellingly, these oocytes have high CDK1 activity yet display little phosphorylation of mitotic substrates, exactly as we observed in *Xenopus* extracts, consistent with a failure to shut off protein phosphatase(s) upon entry into M-phase (*20*). The Gwl-ARPP-Ensa module appears to be active in human cells, because reduction of Gwl levels by RNAi blocks cells in G2 phase of the cell cycle (*22*).

It is still hard to understand the details of how gradually accumulating cyclin levels are converted into the sharp activation of MPF at the G2 to M transition. Gwl appears to require activation by MPF (*11*), and once it is turned on, it phosphorylates Ensa, which in turn switches off PP2A-B55δ (Fig. 4). This promotes the activation of

MPF, by increasing phosphorylation of Wee1, Myt1 and Cdc25, and it also assists entry into mitosis by reducing the dephosphorylation of MPF targets,. This is an example of a "coherent feedforward loop" (*23*) because Cdk1 phosphorylates its own activation module in a positive feedback loop, it phosphorylates its mitotic target proteins, and it indirectly inactivates the antagonising protein phosphatase by activating Gwl and the downstream phosphatase inhibitor, Ensa. Clearly, once this system is active, the cell switches completely into mitosis in a kind of latch mechanism. Thus, both Gwl and Ensa are essential for the maintenance of the mitotic state, implying that inhibition of protein phosphatases is critically important for this. How the return to interphase is brought about is unclear. When cyclins are degraded and Cdk1 levels fall, Gwl and Ensa are dephosphorylated, presumably by protein phosphatase(s) other than PP2A-B55δ, such as PP1(*24, 25*). The threshold for activation of Gwl and entry into mitosis depends on the balance of activities of these as-yet unidentified phosphatases and that of MPF.

**Acknowledgements**

Thanks to H. Mahbubani, J. Kirk and L. Egbuniwe for care of frogs, and other members of the laboratory for advice and reagents, especially J. Gannon for the antibody to doubly phosphorylated $Thr^{14}$-$Tyr^{15}$ of Cdk1 (CP 3.2). SM was supported by a fellowship from the Japan Society for the Promotion of Science.

**Figure legends**

**Fig. 1** Ensa and ARPP-19 are substrates of Gwl. **(A),** Phosphorylation of two small proteins in *Xenopus* interphase egg extract to which Gwl was added. Coomassie blue staining (right panel) and autoradiography (left panel). The positions of the two candidates and of Gwl are indicated with arrows and an arrowhead, respectively. **(B)**, *In-vitro* phosphorylation of candidate substrates by Gwl. Lanes marked 'Mw' are molecular size markers. **(C),** Sequence alignment of *X. laevis* Ensa and ARPP-19. Conserved residues are shown in red. **(D),** *In vitro* phosphorylation of Ensa by Gwl. Wild type Ensa and mutants were phosphorylated by Gwl kinase (upper panel), CDK (middle panel) or PKA (lower panel). In the 7A mutant, $Ser^{2}$, $Thr^{28}$, $Ser^{51}$, $Ser^{67}$, $Thr^{93}$, $Thr^{99}$ and $Ser^{109}$ of Ensa were all substituted by alanine. In the 6A mutants, one of these 7 residues was restored to its original state as indicated.

**Fig. 2** Regulation of PP2A-B55δ by Ensa. (**A),** Phosphatase activities of recombinant PP2A-C monomer, AC dimer and AB55δC trimer complexes were analyzed with and without Ensa using $^{32}PO_4$-labeled maltose binding protein fused to a 25-residue peptide containing $Ser^{50}$ of Fizzy (MBP-Fizzy-Ser50) as substrate (*10*). Results are the means ± range for three experiments. The activities are expressed as % of controls. Open bar; buffer, grey bar; Ensa, black bar; Ensa thiophosphorylated by Gwl. **(B),** Physical interaction between Ensa and PP2A subunits in *Xenopus* interphase egg extract. Fractions bound to (lanes 5-7) and not retained (lanes 2-4) by Ensa beads were analysed for PP1, PP2A and PP5 subunits.

**Fig. 3** Phosphorylation and function of Ensa in *Xenopus* egg extracts **(A),** Proteins from *Xenopus* egg extracts arrested in the indicated cell cycle stages were

supplemented with or without his-tagged recombinant wild type or S67A mutant Ensa. Recombinant (added) or endogenous Ensa was detected by immunoblotting with anti-Ensa (upper panel) or anti-phospho-Ser$^{67}$ (middle panel) antibodies. The same set of samples was also analyzed by SDS-PAGE in the presence of Phos-tag™ (lower panel). The migration positions of dephosphorylated (Ensa-OH, Added-OH or Gwl-phosphorylated (Ensa-$PO_4$, Added-$PO_4$) proteins are shown. **(B),** Endogenous Ensa was immunodepleted (lane 2) from fresh 'cycling' extract and either wild type (lane 3) or S67A mutant (lane 4) of recombinant Ensa added back. **(C-E),** Egg extracts shown in (B) were incubated at 23°C and aliquots were taken at 7-minute intervals for analysis. Apc3 (upper panel), cyclin B2 (middle) and phosphorylation of Tyr$^{15}$ of Cdc2 (lower) were detected by immunoblotting. Histone H1 kinase (black squares in the graphs) and MBP-Fzy-Ser$^{50}$ phosphatase activities (red circles) were measured and plotted (70 minutes of H1 kinase and 0 minute of Ser$^{50}$ phosphatase activities of mock extract taken as 100%). (C), mock depletion; (D), Ensa depleted; (E), Ensa depleted with wild type Ensa added back. See Fig. S3 for additional data from this experiment.

**Fig. 4** A diagram of how PP2A-B55δ is inactivated by CDK via the Gwl and Ensa pathway. Pathways in blue are active in interphase, pathways in red denote those active during mitosis.

**References**

1. D. O. Morgan, *The cell cycle: principles of control*. Primers in biology (New Science Press, London, 2007), pp. 297.

2. A. Lindqvist, V. Rodriguez-Bravo, R. H. Medema, The decision to enter mitosis: feedback and redundancy in the mitotic entry network. *J Cell Biol* **185**, 193 (Apr 20, 2009).
3. A. Kumagai, W. G. Dunphy, Regulation of the cdc25 protein during the cell cycle in Xenopus extracts. *Cell* **70**, 139 (Jul 10, 1992).
4. P. R. Mueller, T. R. Coleman, W. G. Dunphy, Cell cycle regulation of a Xenopus Wee1-like kinase. *Mol Biol Cell* **6**, 119 (Jan, 1995).
5. S. Y. Kim, E. J. Song, K. J. Lee, J. E. Ferrell, Jr., Multisite M-phase phosphorylation of Xenopus Wee1A. *Mol Cell Biol* **25**, 10580 (Dec, 2005).
6. S. L. Harvey, A. Charlet, W. Haas, S. P. Gygi, D. R. Kellogg, Cdk1-dependent regulation of the mitotic inhibitor Wee1. *Cell* **122**, 407 (Aug 12, 2005).
7. G. Pal, M. T. Paraz, D. R. Kellogg, Regulation of Mih1/Cdc25 by protein phosphatase 2A and casein kinase 1. *J Cell Biol* **180**, 931 (Mar 10, 2008).
8. S. Mochida, S. Ikeo, J. Gannon, T. Hunt, Regulated activity of PP2A-B55 delta is crucial for controlling entry into and exit from mitosis in Xenopus egg extracts. *EMBO J* **28**, 2777 (Sep 16, 2009).
9. P. V. Castilho, B. C. Williams, S. Mochida, Y. Zhao, M. L. Goldberg, The M phase kinase Greatwall (Gwl) promotes inactivation of PP2A/B55delta, a phosphatase directed against CDK phosphosites. *Mol Biol Cell* **20**, 4777 (Nov, 2009).
10. S. Mochida, T. Hunt, Calcineurin is required to release Xenopus egg extracts from meiotic M phase. *Nature* **449**, 336 (Sep 20, 2007).
11. J. Yu, Y. Zhao, Z. Li, S. Galas, M. L. Goldberg, Greatwall kinase participates in the Cdc2 autoregulatory loop in Xenopus egg extracts. *Mol Cell* **22**, 83 (Apr 7, 2006).
12. S. Vigneron *et al.*, Greatwall maintains mitosis through regulation of PP2A. *EMBO J* **28**, 2786 (Sep 16, 2009).
13. P. Cohen, A. Knebel, KESTREL: a powerful method for identifying the physiological substrates of protein kinases. *Biochem J* **393**, 1 (Jan 1, 2006).
14. J. A. Girault, A. Horiuchi, E. L. Gustafson, N. L. Rosen, P. Greengard, Differential expression of ARPP-16 and ARPP-19, two highly related cAMP-regulated phosphoproteins, one of which is specifically associated with dopamine-innervated brain regions. *J Neurosci* **10**, 1124 (Apr, 1990).
15. A. Virsolvy-Vergine *et al.*, Endosulfine, an endogenous peptidic ligand for the sulfonylurea receptor: purification and partial characterization from ovine brain. *Proc Natl Acad Sci U S A* **89**, 6629 (Jul 15, 1992).
16. L. Gros *et al.*, Localization of alpha-endosulphine in pancreatic somatostatin delta cells and expression during rat pancreas development. *Diabetologia* **45**, 703 (May, 2002).
17. I. Dulubova *et al.*, ARPP-16/ARPP-19: a highly conserved family of cAMP-regulated phosphoproteins. *J Neurochem* **77**, 229 (Apr, 2001).
18. E. Kinoshita, E. Kinoshita-Kikuta, K. Takiyama, T. Koike, Phosphate-binding tag, a new tool to visualize phosphorylated proteins. *Mol Cell Proteomics* **5**, 749 (Apr, 2006).
19. G. Goshima *et al.*, Genes required for mitotic spindle assembly in Drosophila S2 cells. *Science* **316**, 417 (Apr 20, 2007).
20. J. R. Von Stetina *et al.*, alpha-Endosulfine is a conserved protein required for oocyte meiotic maturation in Drosophila. *Development* **135**, 3697 (Nov, 2008).

21. D. Drummond-Barbosa, A. C. Spradling, Alpha-endosulfine, a potential regulator of insulin secretion, is required for adult tissue growth control in Drosophila. *Dev Biol* **266**, 310 (Feb 15, 2004).
22. A. Burgess *et al*., Loss of human Greatwall results in G2 arrest and multiple mitotic defects due to deregulation of the cyclin B-Cdc2/PP2A balance. *Proc Natl Acad Sci U S A* **107**, 12564 (Jul 13, 2010).
23. S. Mangan, A. Zaslaver, U. Alon, The coherent feedforward loop serves as a sign-sensitive delay element in transcription networks. *J Mol Biol* **334**, 197 (Nov 21, 2003).
24. K. Ishii, K. Kumada, T. Toda, M. Yanagida, Requirement for PP1 phosphatase and 20S cyclosome/APC for the onset of anaphase is lessened by the dosage increase of a novel gene sds23+. *EMBO J* **15**, 6629 (Dec 2, 1996).
25. J. Q. Wu *et al*., PP1-mediated dephosphorylation of phosphoproteins at mitotic exit is controlled by inhibitor-1 and PP1 phosphorylation. *Nat Cell Biol* **11**, 644 (May, 2009).
26. K. Ohsumi, T. M. Yamamoto, M. Iwabuchi, Oocyte extracts for the study of meiotic M-M transition. *Methods Mol Biol* **322**, 445 (2006).

Supplementary Material

## Methods

### Reagents

Phos-tag™ acrylamide was purchased from Phos-tag.com. Okadaic acid (potassium salt) from LC laboratory. Adenosine-5′-(4-fluorosulfonylbenzoate) hydrochloride from SIGMA. Protein kinase A and Amylose resin were obtained from New England Biolabs, and Ni-NTA Agarose from QIAGEN.

### Preparation of *Xenopus* egg extracts

See Mochida and Hunt 2007(*10*) and Ohsumi 2006(*26*) for details of preparation of frog eggs and cell-free extracts.

### Protein phosphatase assays

See Mochida and Hunt 2007 (*10*). In Fig. 2A, the concentration of phosphatases and Ensa in the final assay mixtures were 70 nM and 160 nM respectively, close to their physiological concentrations.

### Protein purification

Purification of rat PP2A-B55δ holo-complex was described by Mochida et al., (*8*). The same strategy was employed to make his-tagged C subunit (β isoform) of PP2A and PP2A core A-C dimer. Maltose-binding protein-fused human cyclin B1 (a.a. 173 to carboxyl terminus) was expressed in bacteria and purified using amylose beads based on a manufacturer's protocol. His-tagged Ensa and ARPP-19 were expressed in bacteria and purified using Ni-NTA agarose beads based on manufacturer's protocol except that bacterial cell pellet was boiled for 5 minutes at 100°C before extraction.

**The modified KESTREL method with FSBA**

The active form of Gwl kinase was immunoprecipitated from mitotic egg extracts for the experiment in Fig. 1a. Interphase egg extracts were passed through PD-10 columns (GE Healthcare) to remove ATP, then supplemented with 10 mM $MgCl_2$ and 1 mM 5'-[p-(fluorosulfonyl)benzoyl]adenosine (FSBA), an ATP analogue which covalently reacts with the ATP binding site of protein kinases and irreversibly suppresses their activity. After incubation for 50 min at room temperature, extracts were passed again through fresh PD-10 columns to remove free FSBA. Sepharose beads carrying Gwl or control beads were incubated with FSBA-treated extracts for 4 minutes at 30 °C in 1x phosphorylation buffer (10 mM Tris-Cl, 50 mM NaCl, 1 mM dithiothreitol, 1 mM EGTA, 0.1 $\mu$M okadaic acid, 40 nM $\gamma$-[$^{32}PO_4$]-ATP, 2 mM $MnCl_2$, pH 7.5). Samples were separated on SDS-PAGE (20% acrylamide) and analysed by autoradiography.

**Purification and identification of Gwl substrates**

FSBA-treated interphase egg extracts were boiled for 5 minutes at 100 °C. These extracts were centrifuged to remove denatured material and the supernatant was used for KESTREL method as described above. The reaction mixture was fractionated by Mono-Q column and peak fractions containing Gwl substrates were analysed by mass spectrometry.

**Mass spectrometry**

Peptides for analysis were generated by *in situ* tryptic digestion of protein/gel bands. LC-MS/MS analysis of the peptides was carried out on a LTQ Orbitrap XL/ETD mass

spectrometer (ThermoScientific, U.S.A) and the data searched against a concatenated, non-redundant protein database (UniProt KB15.5), using the Mascot search engine (Matrix Science, U.K.).

**Antibodies and immunodepletion**

*Xenopus* Ensa cDNA was amplified from an egg cDNA library using oligos 5'-gatgtcggataaatacatagg-3' and 5'-ttagacgtggtgcaagtcctcg-3'. The 8xHis tagged protein was expressed in bacteria and purified using Ni-NTA agarose (QIAGEN) for injection into rabbits. Antisera were affinity-purified using a column of covalently bound GST-Ensa. For immunodepletion, antibodies were conjugated to protein A-Sepharose beads (SIGMA). His-tagged *Xenopus* Gwl was expressed in bacteria and used as an antigen to make polyclonal rabbit antibodies. Anti-Ensa phospho-Ser67-specific antibody was raised against a synthetic peptide, CQKYFDSpGDYN (where Sp denotes phosphorylated serine).

**Physical interaction between Ensa and endogenous PP2A**

Glutathione S-transferase-fused Ensas (hypo-, Gwl- or PKA-thiophosphorylated) were covalently conjugated to cyanogen bromide-activated Sepharose 4B beads. The beads were incubated with interphase egg extract for 10 minutes and unbound and bound fractions were analysed by immunoblotting for the indicated PP2A subunits, and PP1 and PP5 catalytic subunits.

**Supplementary figure 1**

ARPP-19 has highly similar properties to Ensa. (**A),** Phosphorylation of ARPP-19 by Gwl, CDK and PKA. Recombinant wild type ARPP-19 or its mutants were

phosphorylated *in vitro* by Gwl (upper panel), CDK (middle panel) or PKA (lower panel). In the 11A mutant, $Ser^{2}$, $Ser^{15}$, $Ser^{28}$, $Ser^{32}$, $Ser^{51}$, $Ser^{67}$, $Ser^{87}$, $Thr^{90}$, $Thr^{93}$, $Thr^{99}$ and $Ser^{109}$ were all substituted with alanine. In the 10A mutants, one of these 11 residues was restored to its original form. **(B),** Phosphatase activities of recombinant PP2A-AC dimer and AB55δC trimer complexes were assayed with and without ARPP-19 using radiolabeled phosphorylated MBP-Fizzy-Ser50 as a substrate. The activities are expressed as % of the buffer controls. Open bar; buffer, grey bar; ARPP-19, black bar; ARPP-19 thiophosphorylated by Gwl. **(C),** ARPP-19 and Ensa do not inhibit PP1 *in vitro*. Phosphatase activities of recombinant PP1 catalytic subunit were analyzed with and without ARPP-19 and Ensa using phosphorylase-a as a substrate. Results are the means ± range for three experiments. The activities are expressed as % of the buffer controls.

**Supplementary figure 2**

The timing of Ensa phosphorylation in relation to other cell cycle regulators. Standard 'cycling' extract was immunoblotted for various proteins and specific phosphorylation sites as indicated on the left: Apc3, Cyclin B2, $Thr^{14}$ & $Tyr^{15}$ of Cdk1, Cdc25, $Ser^{287}$ of Cdc25, Wee1A, Ensa (using a Phos-Tag™ polyacrylamide gel), $Ser^{67}$ of Ensa and Gwl. Histone H1 kinase activity is displayed in the graph.

**Supplementary figure 3**

Ser67 of Ensa is crucial for proper cell cycle progression. **(A),** Endogenous Ensa was immunodepleted from fresh 'cycling' extract and recombinant Ensa S67A mutant was added. This experiment was done at the same time and samples were analysed in the

same way as Fig. 3(C-E). **(B-E),** Wee1A, Cdc25 and the phosphorylation of CDK target proteins were analysed by immunoblotting. Samples were identical to those shown in Fig. 3C-E and Fig. S3A. (B), mock depletion; (C), Ensa depleted; (D) Ensa depleted and wild-type recombinant Ensa added; (E) Ensa depleted with recombinant Ensa S67A mutant added.

**Supplementary figure 4**

Ensa thiophosphorylated by Gwl promotes mitotic phosphorylations. Interphase egg extract was supplemented with a small amount of stable cyclin B and increasing amounts of Ensa (0, 160, 320, 640 or 1280 nM from left to right). Lanes 1 and 2 indicate control interphase and mitotic extracts. Mock-thiophosphorylated Ensa was added to lanes 3-7; Gwl-thiophosphorylated Ensa to lanes 8-12; and PKA-thiophosphorylated Ensa to lanes 13-17.

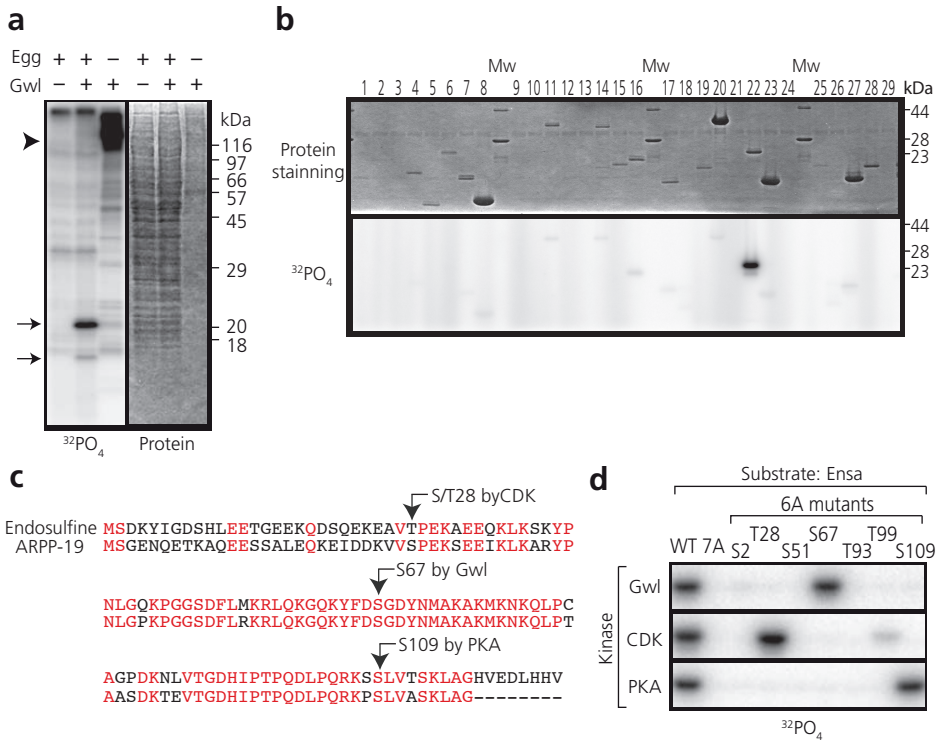


Mochida et al. Figure 1

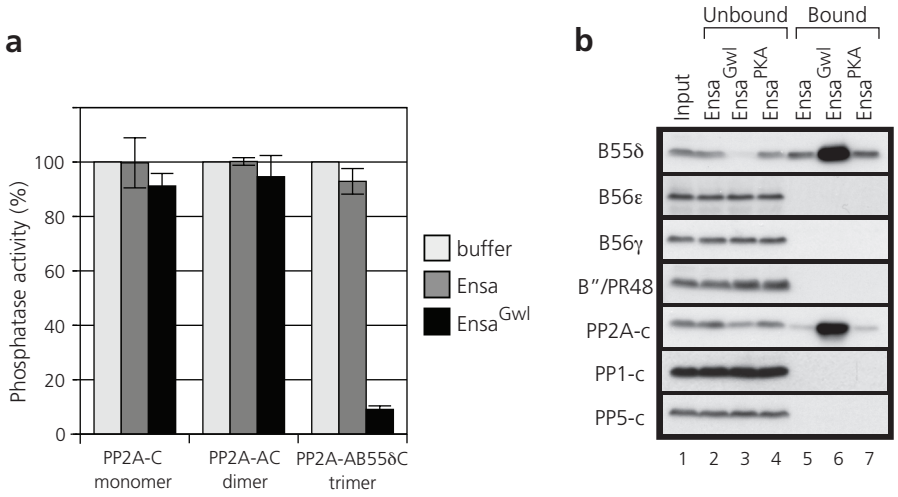


Mochida et al. Figure 2

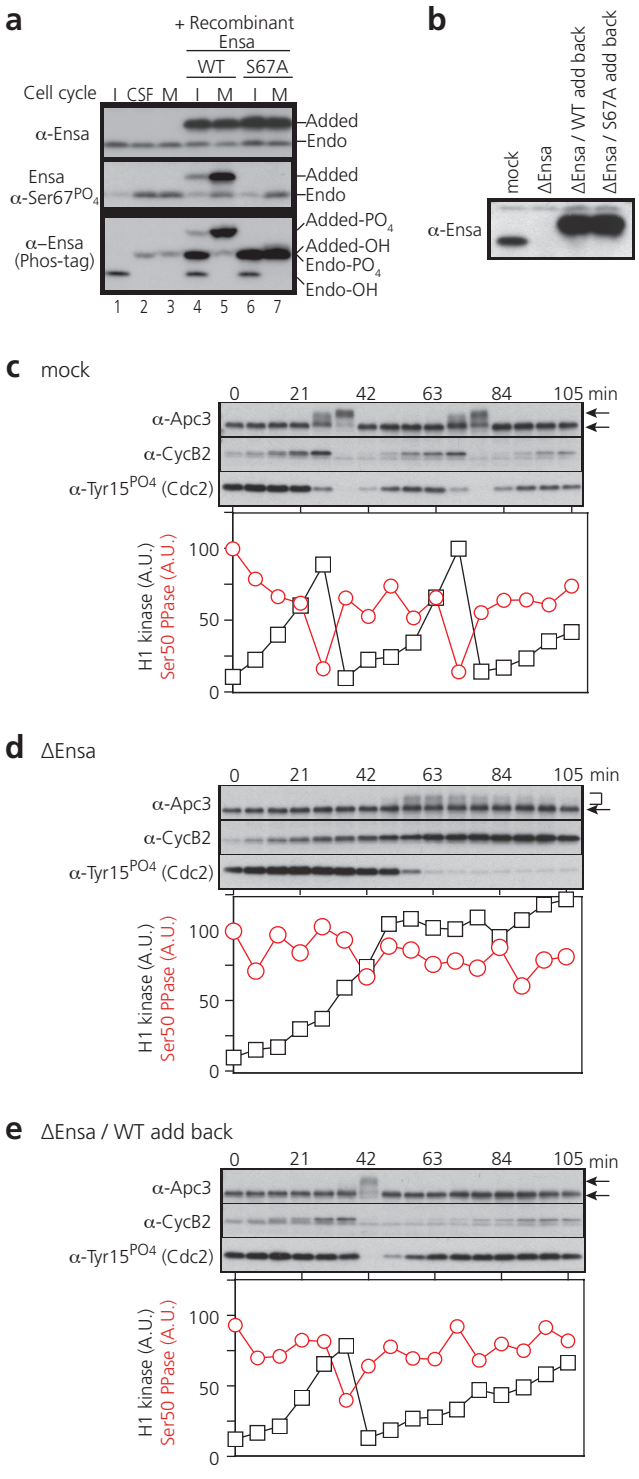


Mochida et al. Figure 3

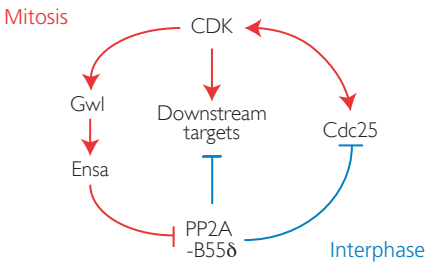


Pathways in red are active in mitosis;
lines in blue are dominant in interphase

Mochida et al. Figure 4

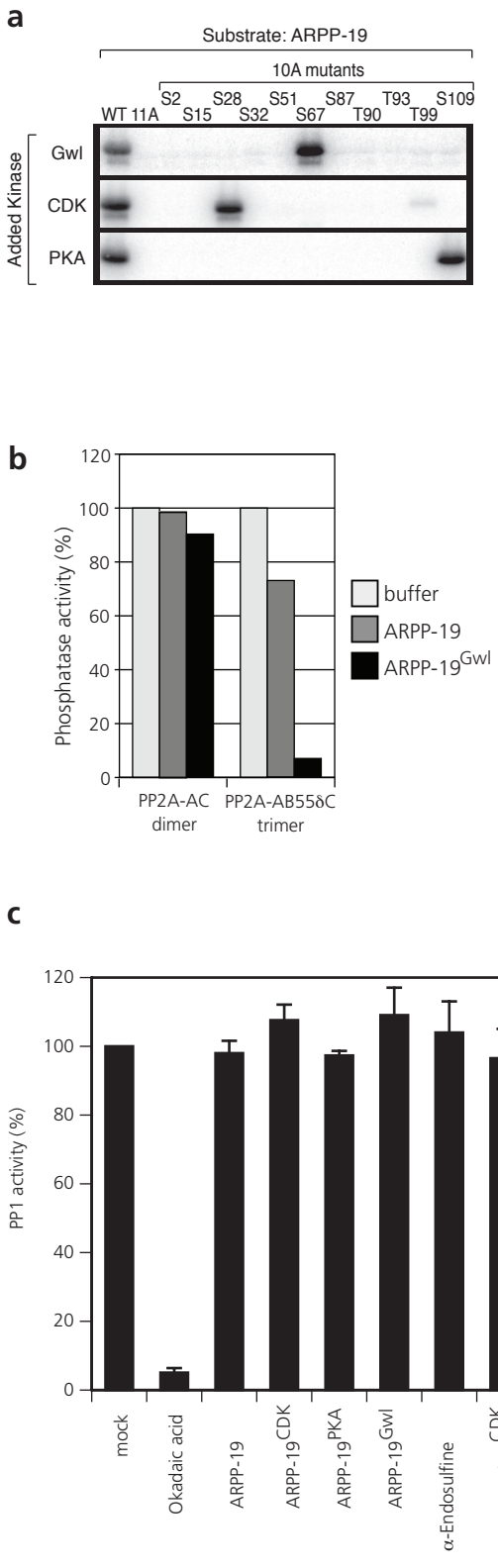


Mochida et al. Supplemental figure 1

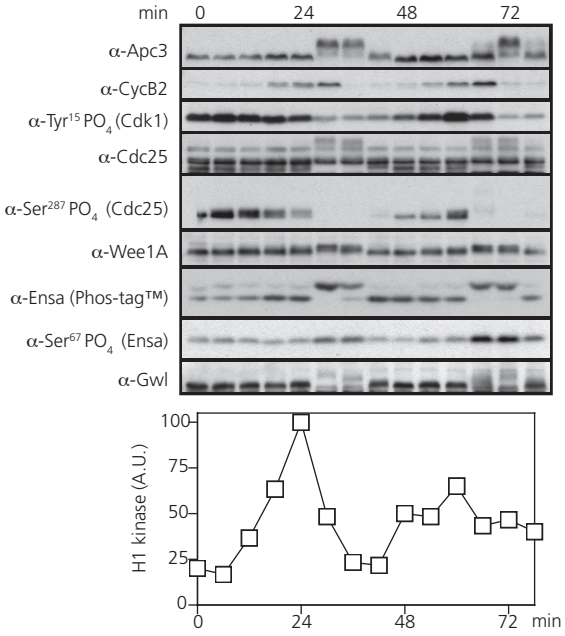


Mochida et al. Supplemental figure 2

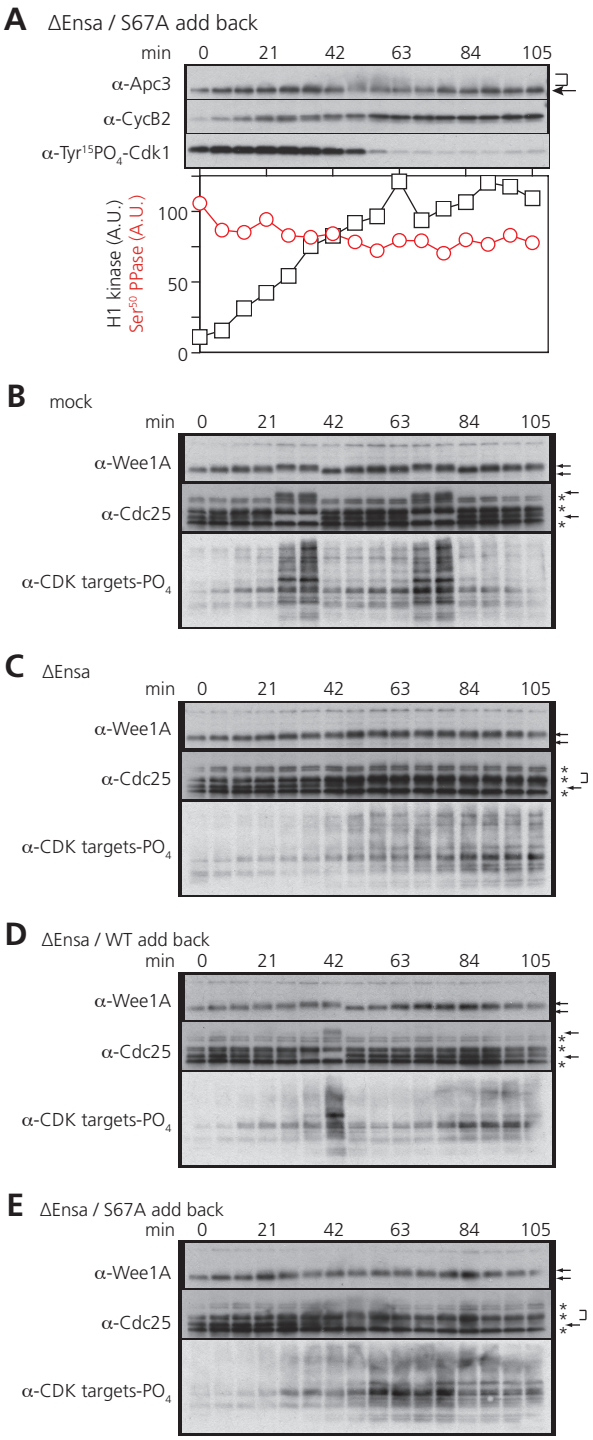


Mochida et al. Supplemental Figure 3

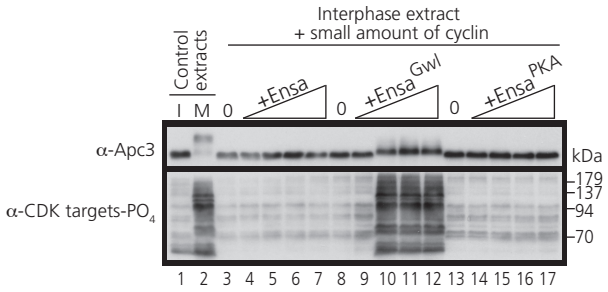


Mochida et al. Supplemental figure 4